DOI 10.14622/Advances_49_2023_19

Influences of mesh and glass surface types on the quality and adhesion of screen-printed elements

Sandra Rosalen and Ulrich Jung

University of Wuppertal, School of Electrical, Information and Media Engineering
E-mails: srosalen@uni-wuppertal.de; ujung@uni-wuppertal.de

Short abstract

This study investigates the impact of mesh screen geometry, surface pre-treatments (hydrophilization and hydrophobization) and the glass side, i.e. air-side or tin-side resulting from the float glass manufacturing process, on the reproduction (line width, roughness and ink thickness) of printed elements in screen printing process and the adhesion of ink on glass. It has been shown that the mesh screen has a stronger influence on the reproduction of the printed elements than the pre-treatment of the glass, and that this has a stronger influence than the side of the float glass. It was also demonstrated that screens with a higher mesh screen (165-030) yield thinner ink films and better adhesion to the glass as compared to screens with a lower mesh screen (120-030).

Keywords: screen printing, float glass, surface treatments, adhesion, reproduction's quality

1. Introduction and background

Screen printing on glass is a widely used method for decorating and functionalizing glass surfaces. The choice of screen and the surface treatment can have a significant impact on the final print quality and ink adhesion. Using a finer mesh screen can result in more precise and detailed prints, while a coarser mesh screen may be more suitable for larger areas or more textured designs. Hydrophilization and hydrophobization are surface treatments that can improve ink adhesion and reduce the amount of ink needed for printing. They are used to change the surface energy of the glass, making it more or less receptive to the ink.

The side of the glass on which the print is applied can also have an impact on print quality. In float glass manufacturing process, the fire side of the glass is formed on the side that faces the flame, while the tin side is formed on the side that faces the tin bath. The tin-side of the glass is usually smoother and has fewer defects than the air-side, which can result in a higher quality print. In some cases, surface defects and roughness can have an impact on ink adhesion. This leads to the common recommendation to use the fire side for sensitive applications.

The aim of the experiments presented here is to understand the influence of these variables (mesh screen, pre-treatment and glass side) on screen printing with UV ink on float glass. For this purpose, solid tone areas and lines were printed on the glass and subsequently the line width, the roughness of the printed area, the thickness of the ink film as well as the adhesion of the ink were measured. These are quality parameters in functional structures. Their variation determines e.g. the resistance or even the proper functioning of displays, integrated smart systems, electronics and components like memories, antennas and batteries.

To reduce the complexity of the experiments, only one type of UV ink was used.

2. Materials and methods

2.1 Materials

The materials used in this work are listed in Table 1.

Table 1: Materials used (Qty. – quantities used per batch)

Material	**Data** (manufacturer between brackets)	**Qty.**
Substrate	Float glass, transparent, size: 120 mm × 50 mm	28
Ink	UVGS/N50 (Sun Chemical)	50 g
Laboratory dishwasher cleaner (LDC)	Powder, mildly alkaline Neodisher Labo GK (Dr. Weigert) surfactant-free, contains phosphate and chlorine (< 30 % / >5 %)	17.2 g
Silylating agent (SA)	1,1,1,3,3,3-Hexamethyldisilazan CAS no.: 999-97-3 (Carl Roth)	600 ml
Cleaning agents	Ethanol 99.9 % CAS-no.: 64-17-5 (Chemsolute)	3 ml
	Distilled water CAS-no.:7732-18-5 (Wittig Umweltchemie)	5 l
Drying agent	Silica gel CAS-no.:1327-36-2 (Carl Roth)	150 g
Adhesive tape	Adhesive 4204 (Tesa) 25 mm wide, 59 µm thickness	-

2.2 Instruments / equipment

The instruments / equipment used in this work are listed in Table 2.

Table 2: Instruments / equipment used

Instruments / equipment	**Data and settings** (manufacturer between brackets)
Screen printer	AT PAB45 (ATMA ESC), snap off: 2 mm, print speed: 30 mm/s, distance to frame: 344 mm left and 183 mm right
Screen 1 (120)	L-120-030-305PW (NBC), frame 30 mm × 30 mm slope, mesh angle 22.5°
Screen 2 (165)	L-165-030-420PW (NBC), frame 30 mm × 30 mm slope, mesh angle 22.5°
Flood squeegee	165 mm wide, angle 0°, micrometer screw setup 7 mm
Print squeegee	145 mm wide, angle 10°, micrometer screw setup 10 mm
UV conveyor dryer	UN50059 (Technigraf)
Washing machine	MMD 37004 (Medion), washing program P2
Magnetic stirrer	PRSM-10HP (Phoenix Instrument)
Desiccator	DN 200 (Duran)
Scanner for image capture s. ISO/IEC 24790:2017	Perfection 4990 PHOTO (Epson), 1 200 dpi, 24 bits, photo modus
Microscope for surface roughness/ink layer thickness measurement	3D laser scanner microscope VK-X160K (Keyence), surface profile modus, standard 1024 × 768 pixel, RDP on, high accuracy quality, double scan off, ND-filter 30 %, noise removal on, image sharpening off, automatic exposure time, gamma correction value 0.45
Peel tester for adhesion measurement	Peel testing machine VPA-2S (Kyowa), pull-off angle 90°, speed 300 mm/min, measuring length 199 mm, start force 0 N
Adhesive tape applicator	(in-house development), applied tape length: 199 mm

2.3 Software

The software used in this work are listed in Table 3.

Table 3: Software used

Software	**Data and settings** (editor / developer between brackets)
TS24790_Tool 1.5.2a	Version 1.5.2a (ISO) for analysis of line elements – ISO/IEC 24790:2017
Epson Scan	Version 1.0 (Epson) for printed elements scanning – ISO/IEC 24790:2017
Image J	Version 1.53k (NHI) section of the ROI in the scanned elements – ISO/IEC 24790:2017
Multi File Analyser	Version 1.3.1.120 (Keyence) for analysis of microscope captured images
VPA	Version 2.3.2 (Kyowa) for adhesion measurement

2.4 Methods

The methods were divided into 3 groups: cleaning of the surface of the float glass plates, modification of the surface of the float glass plates and analysis of the printed elements. The first two methods were presented in a previous study (Patejdl, Jung and Freieck, 2022) and demonstrate high repeatability.

2.4.1 Cleaning of the surface of the float glass plates (Hydrophilization – HI)

Glass is naturally hydrophilic, which means it has a high surface energy that tends to make it more prone to environmental contamination. Thus, it is necessary to clean them to achieve a homogenous and comparable surface properties, as manufacturing and cutting processes deposit contaminants on the surface. The cleaning procedure requires immersing the plates in a 60 °C distilled water bath with LDC for 60 minutes. The bath should be stirred continuously. The plates are then washed with distilled water with the program P2 in the washing machine (wash at 50 °C, rinse at 65 °C and dry for one hour). Then the glasses were stored in dustproof containers for 1 week.

2.4.2 Modification of the surface of the float glass plates (Hydrophobization – HO)

Surface hydrophobization was performed with hexamethyldisilazan (HMDS), that has two well-known mechanisms to modify the surface. Firstly, it reacts with the adhered water molecules on the glass surface and thus removes the water layer. Secondly, it binds to the now free oxygen atoms of the silicon oxide on the glass surface and thus prevents a further build-up of water from the air on the glasses surface (Shen, et al., 2012).

The hydrophobization is applied as a multistep process and consists first of placing the cleaned glass plates (s. 2.4.1) in an HMDS bath (80 °C) for one hour. After the glasses were cleaned with a cleanroom cloth (Vipers PC 68) with approx. 3 ml ethanol 99.9 % (two repetitions) and placed for one hour under vacuum in a silica gel desiccator and then rinsed in the P2 program described above. At last the glasses were stored in dustproof containers.

2.4.3 Analysis of the printed elements

The printed test chart has lines with widths of 63, 126, 189, 252 and 315 µm printed vertically and horizontally in relation to the squeegee direction (Figure 1a) and a solid tone area of 60 mm × 30 mm printed vertically in relation to the squeegee direction (Figure 1b). The borders of the figures represent the float glass plate.

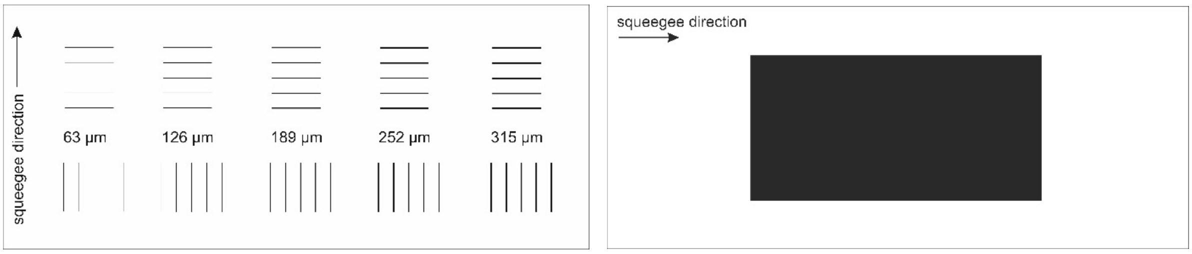

a) *b)*

Figure 1: Printed elements: lines (a) and solid tone printed area (b)

The measurement of line width is a crucial factor in evaluating the accuracy of ink transfer and identifying any variations in ink spread that may arise due to differences in glass sides or surface modifications. The standard ISO/IEC 24790:2017 (International Organization for Standardization, 2017) is typically utilized for measuring line widths in digital printing systems, but it can also be applied to screen printing, as demonstrated in experiments.

The evaluation of the line reproduction based on the ISO/IEC 24790:2017 is calculated using the reflectance ρ. The maximum reflectance (substrate) and minimum reflectance (100 % printed black) are determined to set the reflectance limits $\rho 70$ and $\rho 10$. These data are used in the description of the different reflection zones for the calculation, for example, of line blurriness and line darkness. The line width is the average width of the printed line. The width is calculated along the line from edge to edge (Equation [1]). LETP means “left edge threshold position”, RETP “right edge threshold position”, both in mm, and k is the dot row within a measuring element (line) to determine a local edge position (Figure 2).

$$\frac{1}{n}\sum_{k=1}^{n}(\mathrm{LETP}) - (\mathrm{RETP}) \qquad [1]$$

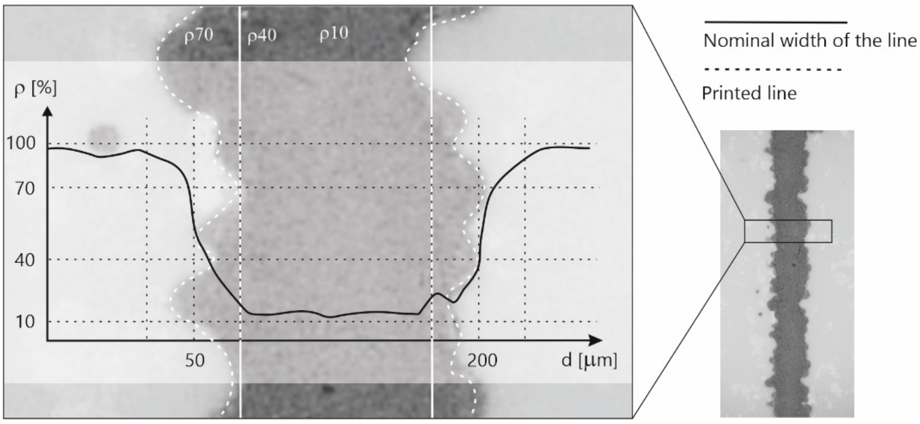

Figure 2: Reflection limits of a printed line according to ISO/IEC 24790:2017 (International Organization for Standardization, 2017) – modified

To determine the thickness and roughness of the ink film, the solid tone printed areas were examined after curing using a 3D laser scanning microscope. For the roughness measurements two parameters, R_z and S_z, were used to quantify roughness, where R_z refers to the 2D with 15 lines spaced 20 pixels apart and S_z measures the 3D areal profile of a 300 µm × 1 046 µm area. Both parameters were calculated by averaging the peak-to-valley height of each sample length. This averaging process ensures that the results are balanced and any isolated high peaks or low valleys along the line or area have minimal impact. The thickness and roughness of the ink film were measured in eight areas, with four located on the edge of the printed rectangle and four in the central section of the printed area (Figure 3).

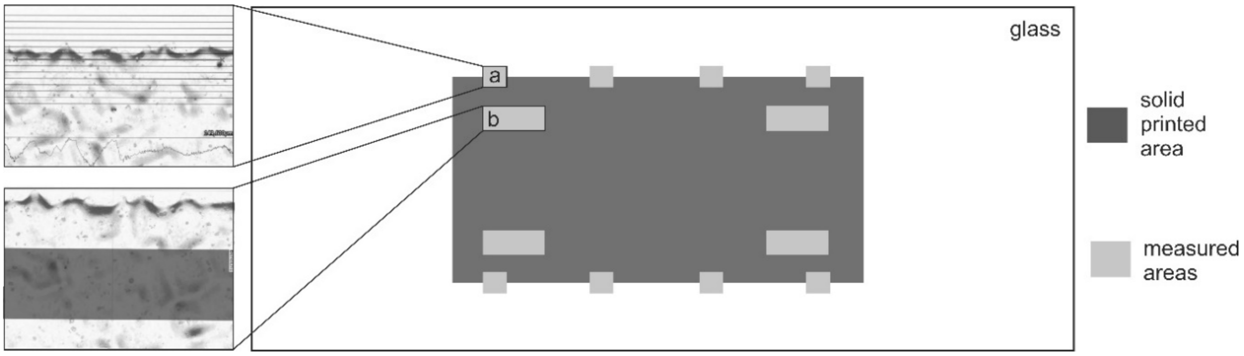

Figure 3: Measured areas and an example of a measurement with lines (a) (R-values) at the edge of the printed area and of an area measurement (b) (S-values) in the internal region of the printed area

Adhesion measurements were conducted in the solid tone printed areas using a peel analyser. The analysis involved applying adhesive tape onto the glass plate with a constant speed and pressure by a special device, and subsequently removing it using the peel analyser. The strength of the adhesion and the degree of delamination of the ink film were both evaluated. These measurements provide key findings into the quality of the ink film and its capacity to adhere to the substrate. In Table 4 are listed the quantity of samples for each analysis, as well as the acronyms used in the following figures and results.

Table 4: Samples quantities and used acronyms (each type indicates both a line width and a printing direction)

Surface modification	Mesh screen	Glass side	Acronyms	Lines (each type / total)	Solid tone areas (edge / central)
Hydrophilization	120-030	air-side	HI-120-AS	25 / 125	120 / 60
		tin-side	HI-120-TS	25 / 125	104 /52
	165-030	air-side	HI-165-AS	25 / 125	120 / 60
		tin-side	HI-165-TS	25 / 125	112 / 56
Hydrophobization	120-030	air-side	HO-120-AS	25 / 125	126 / 68
		tin-side	HO-120-TS	25 / 125	112 / 56
	165-030	air-side	HO-165-AS	25 / 125	112 / 56
		tin-side	HO-165-TS	25 / 125	112 / 56

3. Results and discussion

The results were analyzed by comparing measurements taken from various factors, including the type of mesh screen used (165 and 120), surface modification (HI and HO), glass side (AS and TS) and printing orientation (vertical [V] and horizontal [H] in relation to the print squeegee). The width of printed lines was also analyzed based on the target and actual values. In the following sections, these results will be presented and discussed for the four quality indicators, namely line width, roughness (R_z and S_z), ink film thickness and adhesion forces.

3.1 Line width

Figures 4 and 5 display the relative deviation between the target and actual values for the measured parameter. It is worth noting that the 63 µm lines on mesh screen 165 could not be measured due to the fine mesh. These lines were dotted (not continuous) instead with a continuous shape, which resulted in the fact software is unable to recognize the line borders and returning a measurement error.

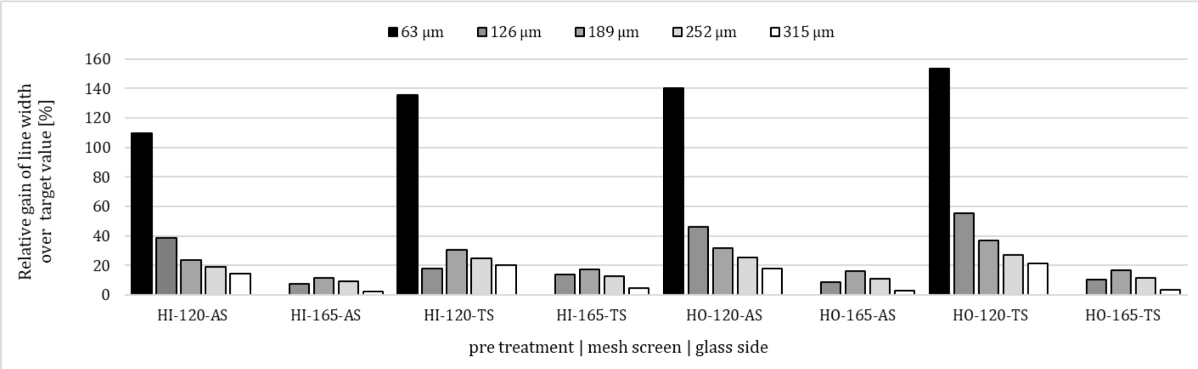

Figure 4: Average relative gain of line width over target value – horizontal direction [%]

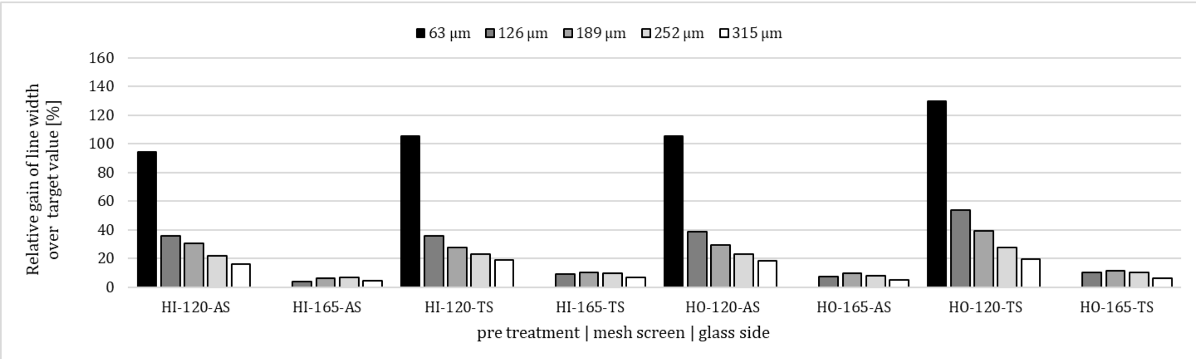

Figure 5: Average relative gain of line width over target value – vertical direction [%]

The deviations from the target value for the lines printed with the 165 mesh are considerably smaller than those of the 120 mesh and this is invariant of the side and treatment of the glass, as well as the printing direction.

In most all cases, measurements show that lines on hydrophilic glass substrates are thinner than their counterparts on hydrophobic glasses. However, this pattern is not observed for the TS 165 samples in the horizontal print direction, where the lines on the hydrophobised glass are actually thinner. This discrepancy could be caused by a distorted preparation process of glass treatment, as this effect is not seen in the vertical orientation. Additionally, the difference in line thickness between hydrophilic and hydrophobic glasses is less pronounced on the 165 mesh than on the 120 mesh. It’s worth noting that the UV ink used in the study tends to spread less on hydrophilic surfaces than on hydrophobic ones. See Figures 6 and 7 for detailed results.

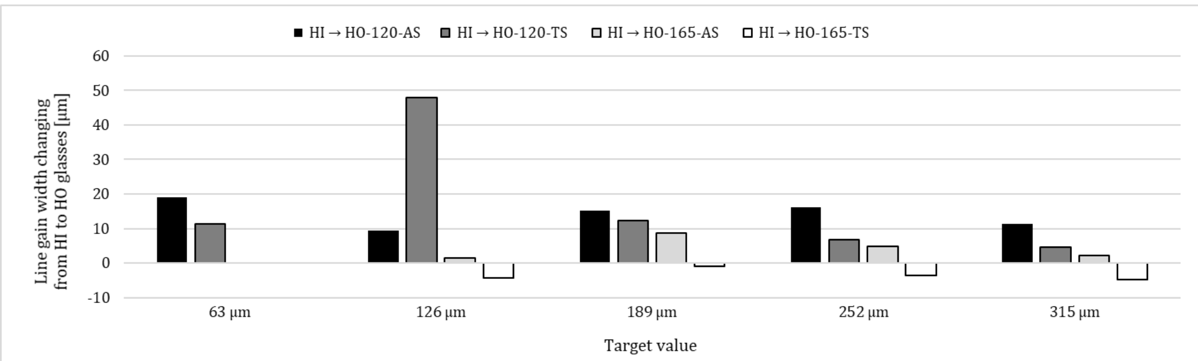

Figure 6: Line gain width changing from HI to HO glasses – horizontal print direction [µm]

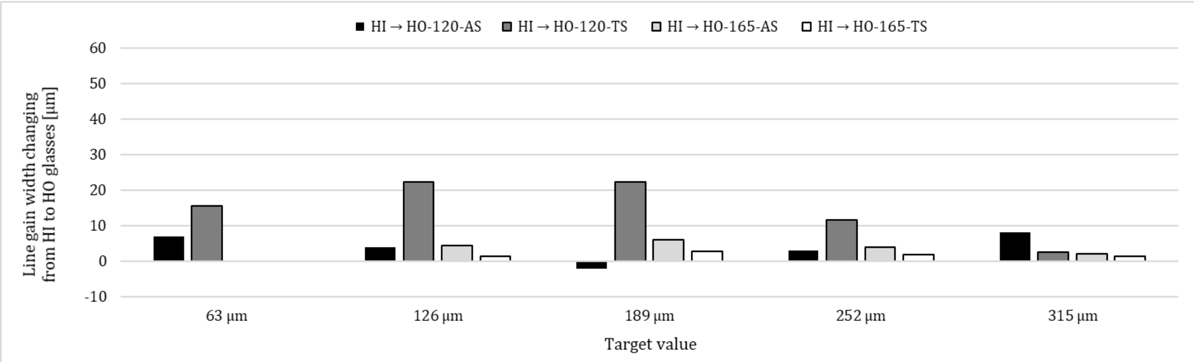

Figure 7: Line gain width changing from HI to HO glasses – vertical print direction [µm]

Lines on the AS are in general thinner than corresponding lines on the glass TS. When comparing the AS and TS side, the horizontal HI-lines exhibit a higher gain in line width than the HO-lines for both 165 mesh and 120 mesh screens. However, the observed line width decrease by the 120 HI-lines when switching from AS to TS (126 µm horizontal and 189 µm vertical, s. Figure 8) is not consistent with the explanations above. It's possible that the glass used in this case contained residues that were not fully removed by the hydrophilization process.

For the vertical lines, a similar trend is seen in the 165 mesh, where the gain is also higher for the HI-lines than the HO-lines. However, the behavior is opposite for the 120 mesh screens. Although lines printed on the TS side are generally thicker, the increase is more significant for the HO-lines. Interestingly, there are two outliers with the HI-120 lines. One outlier is smaller, in the vertical direction at 189 µm nominal line width, where the average TS value is 6.19 µm smaller than the AS value. The other outlier is larger, at 126 µm horizontally, with a difference of 26.31 µm. Figure 7 illustrates these points, where the 126 µm outlier being particularly prominent.

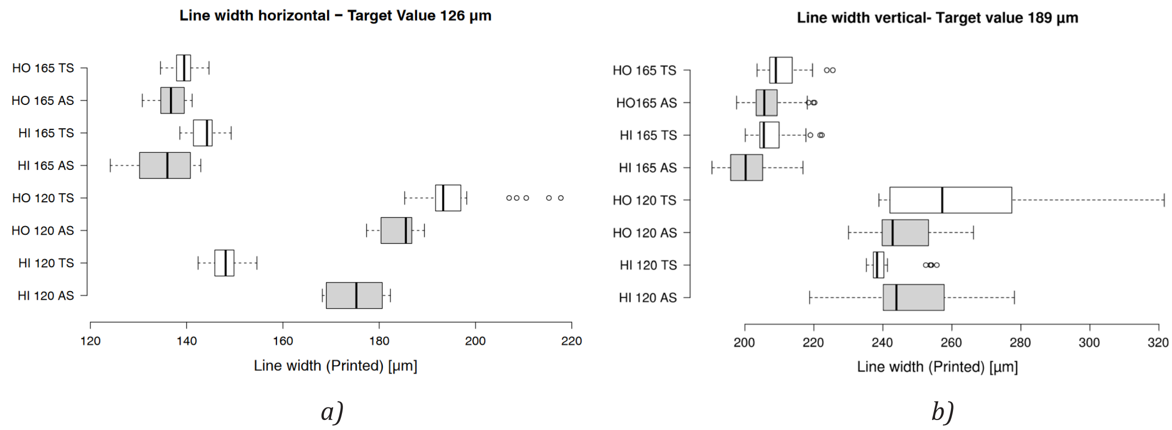

Figure 8: Line width 126 µm horizontal (a) and 189 µm vertical (b)

Figure 9 shows how large horizontal lines are compared to their vertical counterparts. Positive values mean that the horizontal lines are larger than the vertical ones. Negative values mean that the average line widths in the horizontal orientation are thinner than in the vertical orientation. It can be seen that lines in horizontal printing orientation tend to deviate less from the target value with increasing line thickness than those in vertical orientation. In the line widths of 63 µm to 252 µm, the average values of the vertical line width are predominantly thinner than those of the horizontal. At 315 µm this is the opposite. These deviations could not be explained through the experiments made in this study.

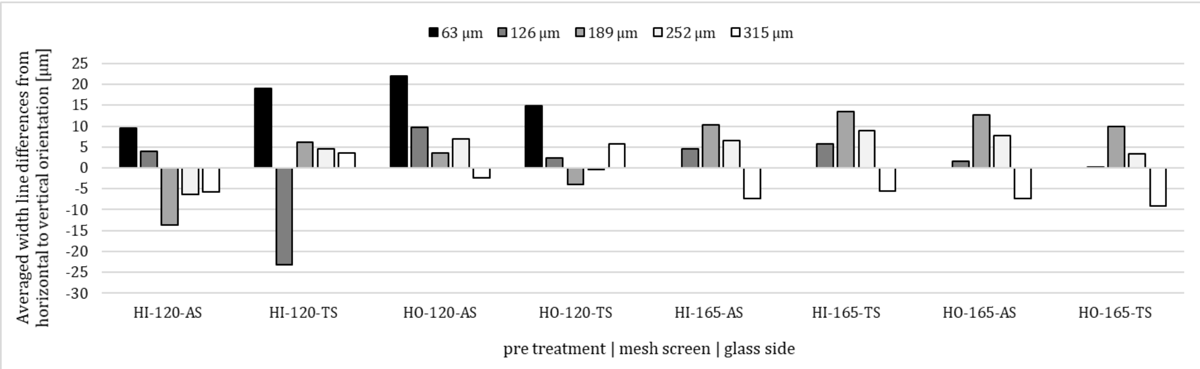

Figure 9: Averaged width line differences from horizontal to vertical orientation [µm]

3.2 Roughness

Line and area roughness of the samples printed with the 165 mesh are significantly lower than those of the 120 mesh across all measurements. An explanation for this result is that the surface roughness of the 165 mesh screen is in itself – due to the higher thread count – lower than that of the 120 mesh screen. Figure 10 shows this as an example using the AS side of the HO-glasses. Both for the measurements of the internal surface and the edges, the largest R_z values of the 165 mesh are smaller than the smallest R_z values of the 120 mesh.

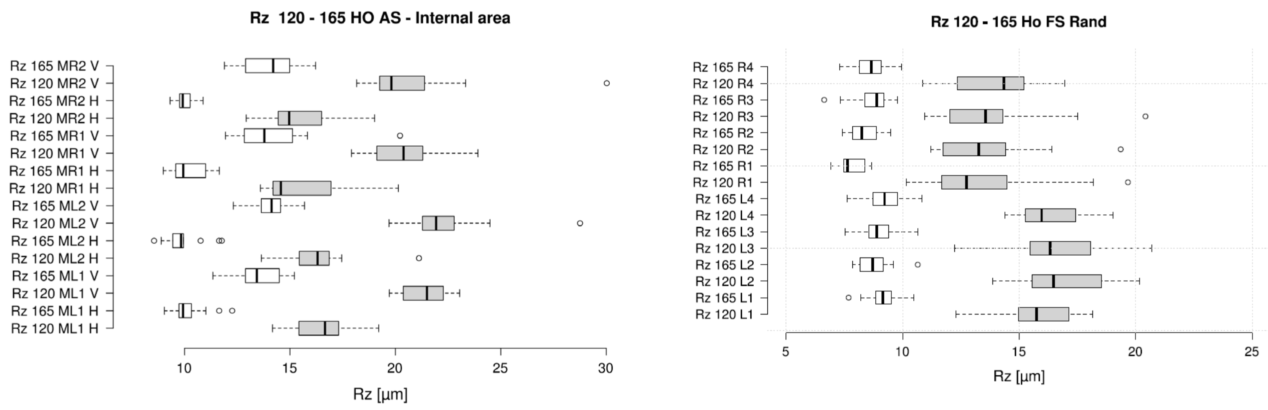

Figure 10: Comparison of the line roughness R_z between the two mesh screens; (a) in the internal areas of the ink layer surface, and (b) at the edges (printed with the 165 mesh on the AS side of the HO-glasses)

The surface roughness difference on the HI-glasses is between the two mesh screens significantly low. Although the R_z values of the 165 mesh are predominantly smaller as well, there are overlaps in the value ranges between the results of the meshes in the boxplots. The diagrams in Figure 11 shows also that the minimum and maximum values of the 165 mesh are lower than those of the 120 mesh.

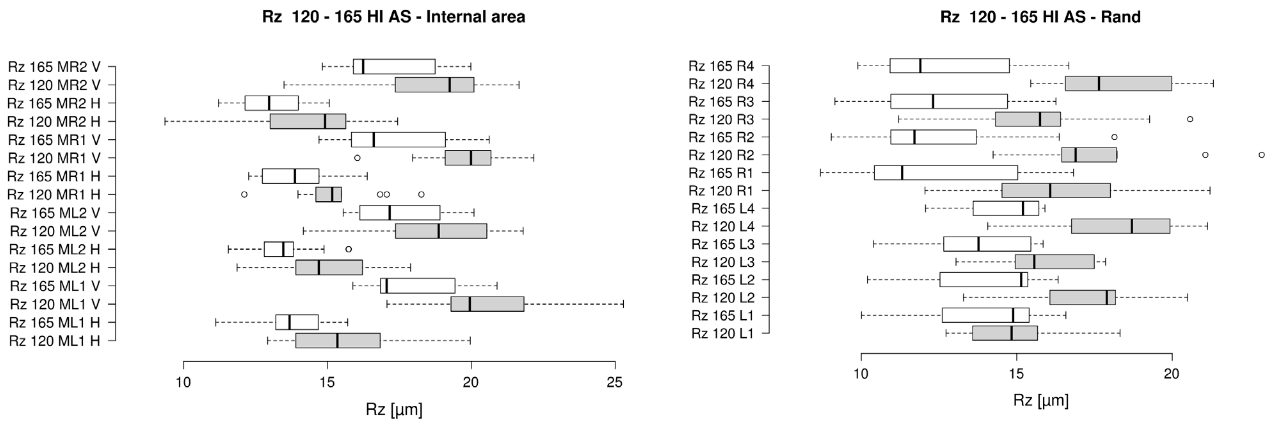

Figure 11: Comparison of the line roughness R_z between the two mesh screens; (a) the internal areas of the ink layer surface, and (b) at the edges (printed with the 120 mesh on the AS side of the HI-glasses)

The S_z values show a similar performance to the R_z values, with a lower standard deviation, which is expected to measurements in areas in relation to measurements on lines (see Table 6).

Comparing the types of pretreatment, it was observed that both mesh screens show quite different behavior when switching from hydrophilic to hydrophobic glasses. In the case of the 120 mesh, the HO-glasses surface is usually slightly rougher on than its HI counterpart. However, there is usually overlap between the R_z measured values of the respective surfaces. A similar result can be seen by the S_z values. Here, too, the values of the HO-glasses are slightly higher, but overall they are quite close to each other. The behavior of the 165 mesh is different. When comparing HO and HI. The R_z values of the HO-glasses are clearly smaller than those of the HI-glasses. This is not so obvious shown by the S_z values. Although the values of the HO-glasses are also lower than those of the HI-glasses.

There are no major differences between AS or TS or even a tendency in either apparent for either HI or HO-Glasses.

3.3 Ink film thickness

According to the literature (Scheer, 2007), ink thickness is primarily dependent on the mesh screen geometry. Other factors such as ink viscosity, squeegee angle and speed have only a secondary influence. The most important parameter here is the theoretical ink volume (V_{th}). Meshes with a larger ink volume also produce a thicker wet ink film on the substrate (Scheer, 2007). Since UV-curing ink was printed, there should only be a small difference of about 2–3 % between wet and dry ink film thickness (Scheer, 2007; Berufsgenossenschaft Energie Textil Elektro Medienerzeugnisse, 2020). The V_{th} of the 120 and 165 meshes are 18.6 cm^3/m^2 and 8.0 cm^3/m^2 respectively. The ink film thickness measurements are presented in the Figure 12.

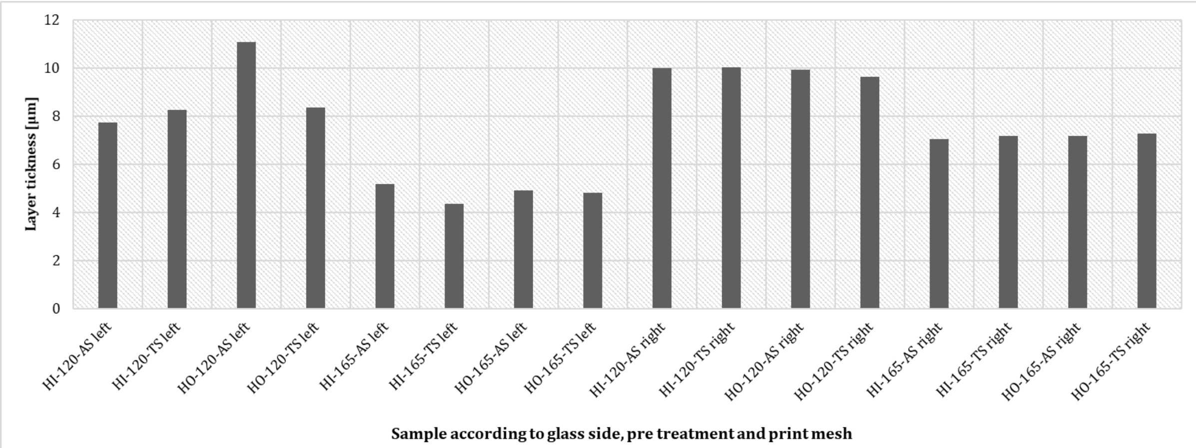

Figure 12: Average ink film thicknesses – right and left side of the solid tone printed area 120 HI AS, 120 HI TS, 120 HO AS, 120 HO TS, 165 HI AS, 165 HI TS, 165 HO AS and 165 HO TS

The results reflect the theoretical assumption. Both on the right and on the left edge side of glass, and widely independent of the type of pre-treatment or the glass side, the results remain constant.

3.4 Adhesion

Figure 13 shows the average peel force required per sample to separate the adhesive tape from the ink layer. Only those specimens were taken into account here in which no delamination (= peeling of the ink layer when the adhesive tape is removed from the glass surface) occurred in the measurement area.

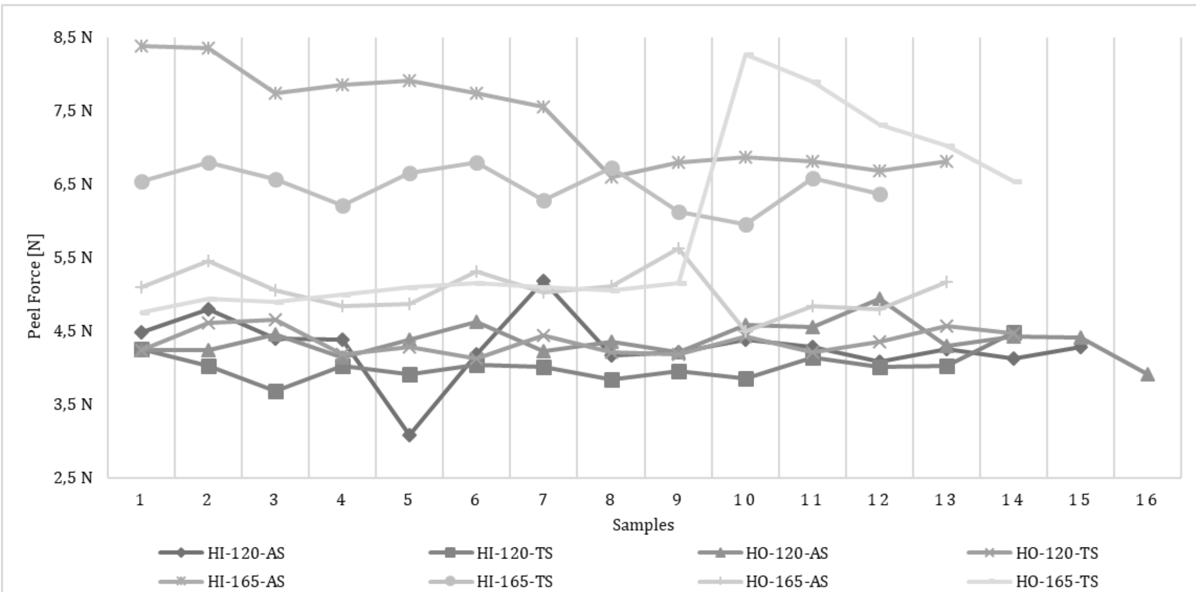

Figure 13: Peeling test – overview of the average peeling force per sample

It can be seen that the specimens printed with the 165 mesh require on average a higher force to trigger the release of the adhesive tape than those printed with the 120 mesh. Table 5 shows the measurements, deviation and delamination (exemplary, Figure 14) of all samples separated by mesh, pre-treatment and glass side.

Table 5: Variation and measurements of the peel test results and delamination (A: number of samples, B: samples with delamination, C: Delamination in % and D: measured points)

Samples	$\bar{x}$ *F* [N]	Min [N]	Max [N]	Range [N]	σ [N]	A	B	C [%]	D
HI-120-AS	4.38	3.77	5.53	1.76	0.31	14	2	14.29	1573
HI-120-TS	4.02	3.16	4.59	1.43	0.21	14	0	0	1694
HO-120-AS	4.43	3.69	5.25	1.56	0.24	17	2	11.76	1452
HO-120-TS	4.36	4.01	4.78	0.77	0.19	14	0	0	1573
HI-165-AS	7.40	6.41	8.70	2.29	0.65	15	2	13.33	1331
HI-165-TS	6.45	5.80	7.02	1.22	0.28	14	2	14.29	1331
HO-165-AS	5.07	4.19	6.04	1.85	0.33	14	3	21.43	1452
HO-165-TS	5.93	4.46	9.10	4.64	1.26	14	0	0	1573

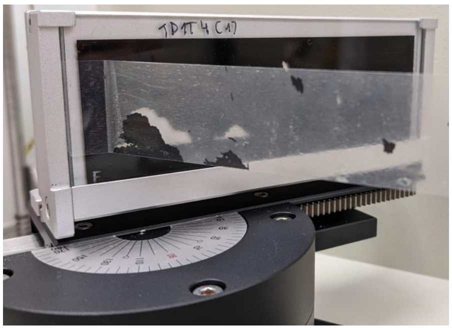

Figure 14: Example of partial delamination

The values of the 120 mesh show only slight variations between the HI and HO-glasses and glass sides (AS/TS). The average peel force ranges from min. 4.02 N to max. 4.43 N. By the 165 mesh varies the average peel force from min. 5.07 N to max. 7.4 N. The average peeling force is also higher for the HI-glasses than for the HO-glasses. In relation to the glass side, there is no clear influence on adhesion.

A possible explanation for the higher peeling forces, and thus also a higher adhesion between the ink surface and the adhesive of the tape, could be found in the different roughnesses of the ink layer produced by the two mesh screens during printing (Figure 15). Depressions appear in the surface which are no longer wetted by the adhesive and thus give rise to air-filled cavities (Habenicht, 2009). The more of these air bubbles are formed per unit area, the more the adhesion effect decreases. Table 6 shows the results. The numerical correlation between roughness and bond strength, in this case was 0.40, this means weak, for both R_z and S_z. The roughness here does not appear to have a preponderant role in the adhesion.

Table 6: Comparison of peel forces to surface roughness

Samples	Average peel force [N]	Average R_z internal area [µm]	Average S_z internal area [µm]
HI-120-AS	4.38	17.24	34.91
HI-165-AS	7.40	15.52	31.83
HI-120-TS	4.02	17.10	33.42
HI-165-TS	6.45	16.67	34.75
HO-120-AS	4.43	18.64	36.37
HO-165-AS	5.07	12.02	29.62
HO-120-TS	4.36	18.42	35.28
HO-165-TS	5.93	12.37	29.74

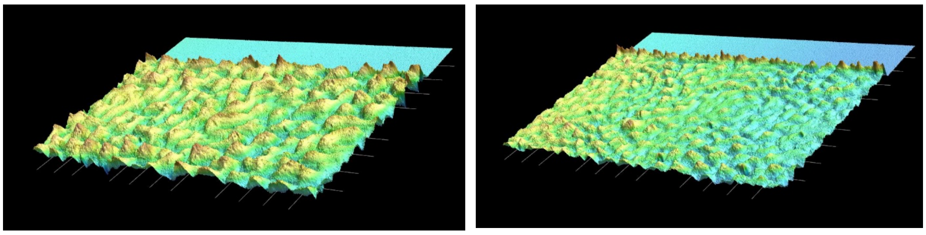

a) b)

Figure 15: Screen print 3D-images of 120 mesh (a) and 165 mesh (b) with 700× magnification

Another possible explanation for the phenomena is that the ink films printed by the 120 mesh are thicker than the films printed by the 165 mesh. Thicker films tend to have a higher curing energy. As the same curing time was used for all specimens, it is possible that the ink film on the 120 mesh is not fully cured. Finally, differences in the so called sweating layer should not show significant dependence on the ink film thickness and therefore could not have a major influence on the adhesion in this case.

4. Conclusions

The experiments presented here aim to understand the factors that influence the print quality of UV ink on float glass. According to the literature, the mesh screen is the factor that most influences the final printing result. This could be verified in the experiments. In summary, in relation to the mesh screens (165 and 120) it can be stated, on the basis of the experiments carried out, that the lines printed with the 165 mesh vary less (smaller delta) from the target value, that the printed surface has less roughness, the thickness of the dry ink film is thinner and the adhesion of the ink is higher than when printed with the 120 mesh. In relation to the surface pretreatment (HO and HI) it was possible to note, that the printed lines on the hydrophilic surfaces had less spreading (thinner lines) and showed higher roughness than those printed on the hydrophobic surfaces. The rise in roughness could not be verified for the 120 mesh. Lines printed on the AS are thinner than those printed on the TS. A clear influence of the glass side on the roughness could not be demonstrated.

In order of influence, it was found that the mesh screen geometry has the stronger influence on the aspects tested here (line reproduction, roughness, ink film thickness and adhesion) than the pre-treatment of the glass, and this in turn has a stronger influence than the side of the float glass.

References

Berufsgenossenschaft Energie Textil Elektro Medienerzeugnisse, 2020. *UV-Trocknung*. [online] BG ETEM. Available at: <https://medien.bgetem.de/medienportal/artikel/TUIwMzQ-/> [Accessed 21 March 2023].

Habenicht, G., 2009. *Kleben: Grundlagen, Technologien, Anwendungen*. 6th ed. Berlin: Springer.

International Organization for Standardization, 2017. *ISO/IEC 24790:2017: Information technology – Office equipment – Measurement of image quality attributes for hardcopy output – Monochrome text and graphic images*. Geneva: ISO.

Patejdl, S., Jung, U. and Freieck, K., 2022. Wetting and adhesion phenomena of surface-treated float glass. In: C. Ridgway, ed. *Advances in Print and Media Technology: Proceedings of the 48th International Research Conference of iarigai*. Greenville, USA, 19–21 September 2022. Darmstadt: iarigai.

Scheer, H.G., 2007. *Siebdruck-Handbuch*. Lübeck: Der Siebdruck, pp. 77–78.

Shen, Q., Chen, X., Guo, J., Taeyu, M., Shi, D., Wang, D., Qu, L., Lu, K., Hou, X., Sun, J. and Wu, T., 2012. P-50: Low K acryl resin as planarization layer on TFT LCD. *SID International Symposium Digest of Technical Papers*, 43(1), pp. 1247–1250. https://doi.org/10.1002/j.2168-0159.2012.tb06024.x.